

STUDIES OF HYDROGEN ADSORPTION ON Ni-MODIFIED MCM-41 MESOPOROUS MATERIALS.

P. M. Carraro^{1,2}, A. A. García Blanco⁴, F.A. Soria³, G. Lener⁴, K. Sapag⁴, G. A. Eimer², M. I. Oliva¹.

1- Instituto de Física Enrique Gaviola (IFEG UNC-CONICET), Medina Allende s/n, C. Universitaria, 5000, Córdoba, Argentina. Tel./fax: + 54 351 433 4051. Email: carraro@famaf.unc.edu.ar

2- Centro de Investigación en Tecnología Química (CITeQ UTN-CONICET), Maestro López esq. Cruz Roja Argentina, C. Universitaria, 5016, Córdoba, Argentina. Tel./fax: +54 0351 469 0585. Email: geimer@scdt.frc.utn.edu.ar

3- Instituto de Investigaciones en Físico Química de Córdoba (INFIQC CONICET-UNC), Medina Allende s/n, C. Universitaria, 5000, Córdoba, Argentina. Tel./fax: + 54 351 4334169. Email: fesoria@fcq.unc.edu.ar

4- Laboratorio de Sólidos Porosos (INFAP CONICET- UNSL), Chacabuco, 917, 5700San Luis, Argentina. Tel./fax: +54 2652 436151, Email: sapag@unsl.edu.ar

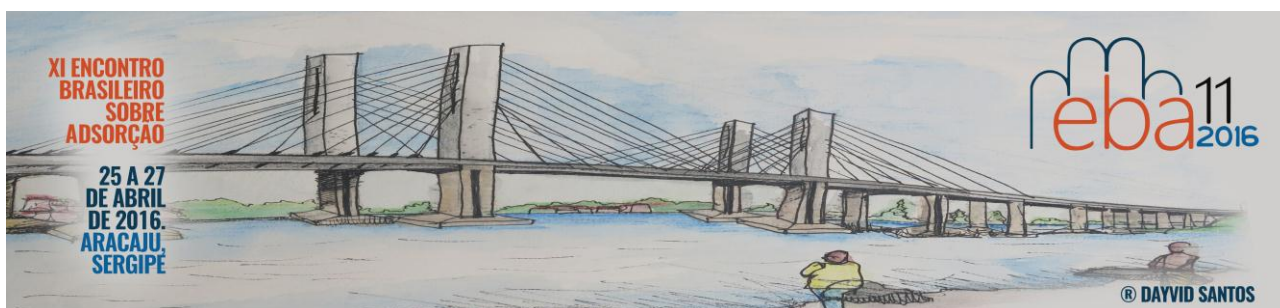
ABSTRACT: MCM-41 mesoporous materials were prepared modified with different Ni contents, as promising materials for hydrogen storage. The final materials were reduced for studying the metallic nickel effect. The Ni/MCM-41 samples were characterized for different experimental techniques such as TPR, XRD and N₂ adsorption-desorption. The hydrogen storage capacity of the materials was evaluated at 77 K and room temperature, and at low and high-pressure conditions respectively. In this study, we focused on the role of dispersed nickel as a way of promoting the interaction with hydrogen as an alternative to improve hydrogen storage materials. The results obtained show that the amount of hydrogen stored was highly enhanced by the dispersion of small amounts of Ni nanoparticles both at 77 and 298 K, indicating that these materials could be used for hydrogen storage in cryogenic and room temperature conditions.

KEYWORDS: Hydrogen storage, nickel, MCM-41, DFT calculations.

1. INTRODUCTION.

The limited fossil fuel resources and the environmental impact of their use require a change to renewable energy sources in the near future (Hirscher 2010). In this context, the hydrogen unlike the fossil fuels is an abundant, clean, and renewable “green” energy carrier. Renewable hydrogen is being widely investigated as a future energy carrier in an effort to reduce greenhouse gas emissions and replace energy production from fossil fuels whose availability is projected to steadily decline in the next few decades. The

development of safe and efficient hydrogen storage technologies for mainly vehicular applications is key for the establishment of a hydrogen-based economy (Yang et al. 2010). However, storing hydrogen efficiently and safely is still a major challenge to realize hydrogen economy. Currently, several methods, including compression method, liquefaction method, and storage in solid materials, have been proposed to store hydrogen. Among these methods, hydrogen storage in sorbents is the most promising technology with respect to efficiency and safety. The two major technologies to store hydrogen in solid materials are chemisorption in the form of metal hydrides and



physisorption of hydrogen on porous materials with large specific surface areas (Züttel 2004; Jena 2011). The essential advantage of physical adsorption storage is reversibility and fast kinetics of hydrogen adsorption in comparison to chemical adsorptions. Nevertheless, it also has the problem of low adsorption enthalpy that results in low storage capacity at ambient conditions.

Mesoporous molecular sieves MCM-41, one member of the M41S mesoporous materials family, has some attributes, such as their high specific surface area, that make them potential candidates for hydrogen storage applications (Park and Lee 2010; Ramachandran, Ha, and Kim 2007).

In this work, ordered mesoporous MCM-41 materials have been synthesized and modified with different Ni loadings by the wet impregnation method. In addition, hydrogen adsorption isotherms at room temperature and high pressures for reduced and un-reduced samples were measured. The characterization of the materials was used in order to interpret the hydrogen adsorption on Ni/MCM-41 materials.

2. MATERIAL AND METHODS

2.1. Synthesis

The pure siliceous mesoporous material (MCM-41) was synthesized as previously reported following the method B (Elías et al. 2009), using cetyltrimethylammonium bromide (CTAB, Merck 99% purity) as template and tetraethoxysilane (TEOS, Aldrich 98%) as silicon source. The MCM-41 material, previously calcined at 773 K for 9 h, was modified with different Ni loadings (2.5 and 10 wt.%) by the wet impregnation method. The MCM-41 was added to an aqueous solution of $\text{Ni}(\text{NO}_3)_2 \cdot 6\text{H}_2\text{O}$ with a concentration corresponding to the desired metallic loading. Then, the water was slowly removed by rotary evaporation at 323 K for about 30 min. The resulting powder was dried at 333 K and then calcined for 9 h at 773 K. The resulting materials were named Ni/MCM-41(x), where x indicates the nominal percentage of metal loading.

These samples were reduced in a H_2 flow. The Ni/MCM-41(2.5) sample was reduced with pure H_2 flow at 723 K and the Ni/MCM-41(10) sample at 873 K for 5 h with a heating rate of 1

K/min. The resulting materials were named: Ni/MCM-41(x)- H_2 , where H_2 indicates that the sample was reduced.

2.2. Characterization

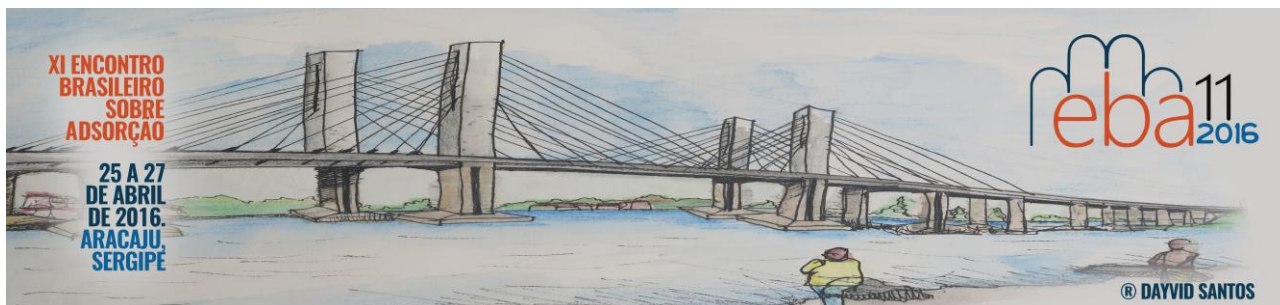
The N_2 adsorption-desorption isotherms at 77 K were measured in a Micromeritics ASAP 2000. The samples were previously degassed at 573 K for 6 h. The specific surface was calculated by the Brunauer-Emmett-Teller (BET) method in the pressure range of P/P_0 : 0.01–0.25. The pore size distributions were determined by Nonlocal Density Functional Theory (NLDFT) method. The X-ray diffraction (XRD) patterns were recorded in a Philips PW 3830 diffractometer with $\text{Cu K}\alpha$ radiation ($\lambda=1.5418 \text{ \AA}$) in the range of 2θ from 1.5 to 7° and from 10 to 80° . The Ni content was determined by Inductively Coupled Plasma Atomic Emission Spectroscopy (ICP) using a spectrophotometer VISTA-MPX CCD Simultaneous ICP-OES-VARIAN. The reducibility of the nickel catalyst was measured by Temperature-Programmed Reduction (TPR) experiments in the Micromeritic ChemiSorb 2720 Instruments. In these experiments, the samples were heated from 298 to 1073 K at a rate of 10 K/min in the presence of 5% H_2/N_2 gas mixture (20 mL/min STP), and the reduction reaction was monitored by the H_2 consumption with a built-in thermal conductivity detector (TCD).

2.3. Adsorption experiments

Hydrogen (99.999%) adsorption capacity at 77 K and pressures up to 10 bar were measured in an automated manometric system ASAP 2050 (Micromeritics Instrument Corporation). High-pressure adsorption isotherms of hydrogen (99.999%) were measured at 293 K in a high-pressure manometric system HPA 100 (VTI Corporation). Previous to all the adsorption experiments, the samples were degassed at 573 K during 5 h under vacuum conditions (5×10^{-3} mmHg).

3. RESULTS AND DISCUSS

3.1. Characterization



The N_2 adsorption-desorption isotherms with their corresponding pore size distribution of the studied materials are shown in Figure 1. The isotherms of all the samples show a characteristic type IV shape according to the IUPAC (Carrott and Sing 1988), typical of well-defined mesoporous structures, with large pore volume and specific area. Moreover, a narrow pore size distribution (PSD) with an average size around 3.5 nm, indicates the uniformity of the pore arrangement (Corma 1997). In all samples, the steep increase of the amount adsorbed at relative pressures around to 0.3 is related to the capillary condensation occurred within the primary mesopores, because the pore size of these materials is nearly 3 nm. All the isotherms show identical shapes, although the adsorption

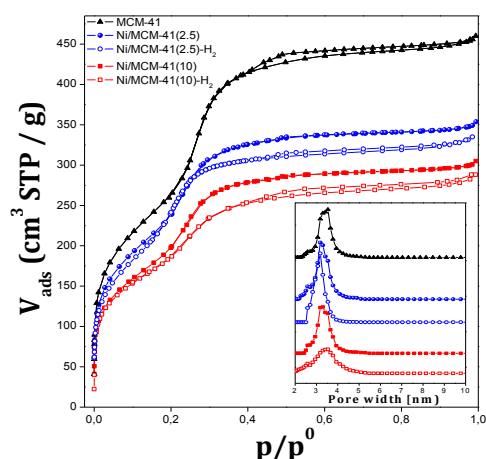


Figure 1. Nitrogen adsorption-desorption isotherms and NLDFT pore size distribution (inset).

capacity decreased with the increase in the nickel loading on the support. This behavior can be attributed to the increased presence of clusters and/or small particles of metal oxides finely dispersed inside the channels as well as large particles on the external surface affects the pore structure and the textural properties of the materials.

Table 1 summarizes the chemical composition and the textural properties. The results show the high area (S_{BET}) of MCM-41, and the

Table 1. Textural properties and chemical composition of the synthesized samples.

| Sample | Area (m^2/g) ^a | Ni (wt.%) ^b | V_{TP} (cm^3/g) ^c |
|-------------------------------|-------------------------------|------------------------|------------------------------------|
| MCM-41 | 940 | - | 0.70 |
| Ni/MCM-41(2.5) | 860 | 2.16 | 0.54 |
| Ni/MCM-41(2.5)-H ₂ | 695 | 8.10 | 0.46 |
| Ni/MCM-41(10) | 837 | - | 0.46 |
| Ni/MCM-41(10)-H ₂ | 650 | - | 0.41 |

^a Determined by BET.

^b Determined by ICP.

^c Pore volume (V_{TP}) determined by N_2 adsorption-desorption

decrease of this parameter (as well as pore volume) due to the presence of nickel in the porous material.

The isotherms of the Ni/MCM-41(2.5)-H₂ and Ni/MCM-41(10)-H₂ samples are nearly similar to the ones of the unreduced samples. Therefore, the ordered pore structure of the unreduced samples is kept after the reductive treatment. A slight decrease in the adsorbed amount (and consequently in the S_{BET}) could suggest some aggregation of the nickel particles subjected to the reductive treatment.

The low-angle X-ray diffraction patterns of the materials studied in this study are shown in Figure 2. All of the samples exhibit a main (100) peak and two weak reflections ascribed to (110)

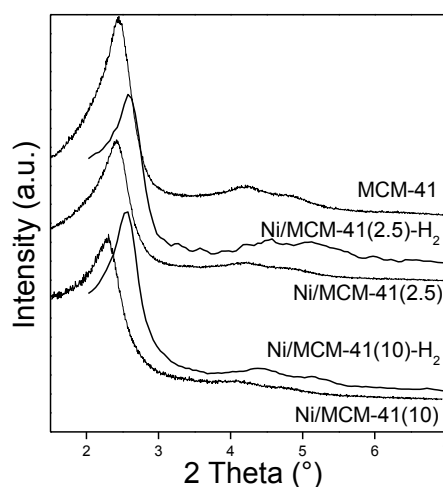


Figure 2. Low-angle XRD patterns of samples.



and (200), which are typical of the MCM-41 mesoporous structures (Do et al. 2005). Those results with N_2 isotherms indicate that the structure was preserved both after the nickel loading as well as after the reduction treatment.

The TPR profiles of the samples are shown in Figure 3, where two reduction regions can be distinguished, one at low-temperatures and other at high-temperatures, which can indicate the reducibility of the metal oxide species with different dispersion and interaction with the support. A first peak appears about 613-673 K, which could be attributed to small amounts of NiO nanoparticles dispersed on the surface and weakly interacting with the framework (Liu et al. 2009). On the other hand, a second peak in the HT region appear at 753-893 K, which can be assigned to smaller NiO clusters or nanoparticles inside the mesoporous channels. Interaction of these NiO clusters or nanoparticles with the support is stronger

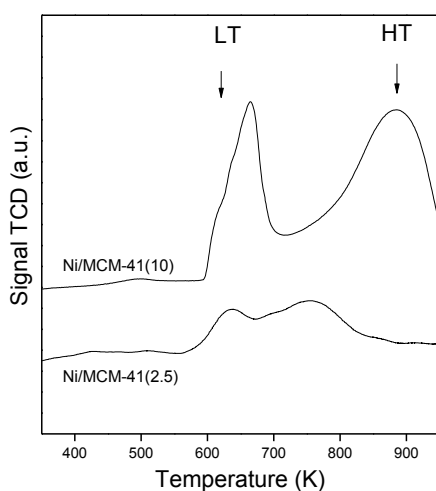


Figure 3. TPR profiles of samples.

and would be finely dispersed inside the mesopores with respect of bigger NiO particles on the external surface (Wu et al. 2011). This peak in this region is more intense and shifts to higher temperature for the higher loaded samples, which would indicate the lower reducibility of these oxide nanoparticles more strongly interacting with the matrix.

3.2. Adsorption experiments

The hydrogen adsorption isotherms at 77 K and pressures up to 10 bar of the unreduced and reduced samples are depicted in Figure 4. Ni/MCM-41(2.5) sample presents the highest H_2 storage capacity, compared with the other samples, giving account of a favourable interaction between H_2 and the nickel species on the surface of that material. In addition, the fact that the reduction treatment did not affect the H_2 adsorption on that material, suggests that the nickel species, which are involved in the enhancement of H_2 adsorption, are perhaps not reducible, maybe because they are

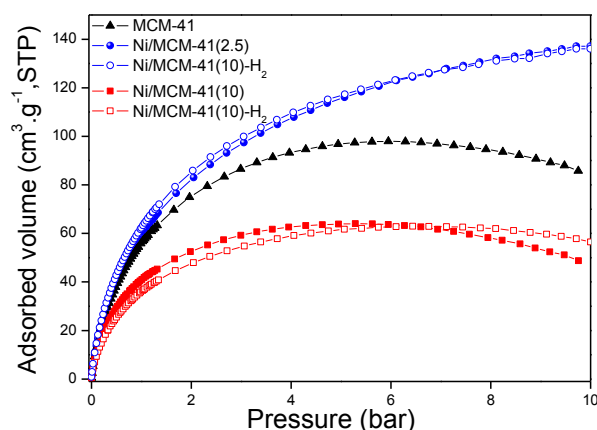
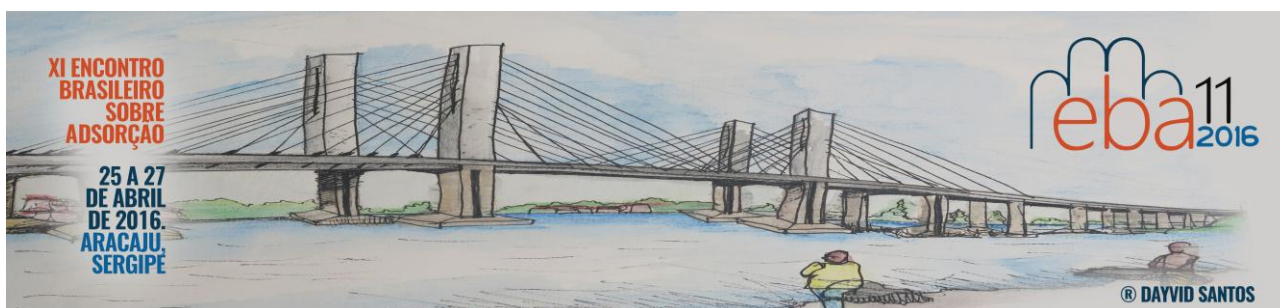


Figure 4. H_2 adsorption-desorption isotherms of the un-reduced and reduced samples, measured at 77 K.

highly dispersed and stabilized by the high interaction between them and the SiO_2 surface. The sample modified with higher nickel loading, even after the reduction treatment, presented lower hydrogen storage capacity at 77 K. Therefore, the adsorption of H_2 at 77 K is not favoured for the high nickel loading (Carraro et al. 2014).

The Figure 5 shows the adsorption isotherms measured at 293 K and up to 40 bar. It can be observed that, the un-reduced Ni/MCM-41 samples store less H_2 than the MCM-41, unlike the behavior shown at 77 K. In addition, the reduced Ni/MCM-41 samples show an important increase in H_2 storage. The fact that unreduced Ni/MCM-41 samples store less H_2 at these conditions could be attributed to an entropic effect due to the increase of the temperature of the system. Under these conditions, the increase of H_2 sorption at the



surroundings of the low coordinated Ni sites, which could explain the behavior of the isotherms at 77 K, would not be favoured because of the high mobility of H₂ molecules at this temperature. In this case, the S_{BET} would be the determinant factor for H₂ storage, explaining why the order of H₂ storage is directly related with the S_{BET} , MCM-41 > Ni/MCM-41(2.5) > Ni/MCM-41(10), for the un-reduced samples.

The reduced Ni/MCM-41 samples show an important increase in the H₂ storage capacity, indicating the appearance of a new mechanism that favours H₂ storage at 293 K in the samples with Ni in its metallic phase, which is not present at 77 K.

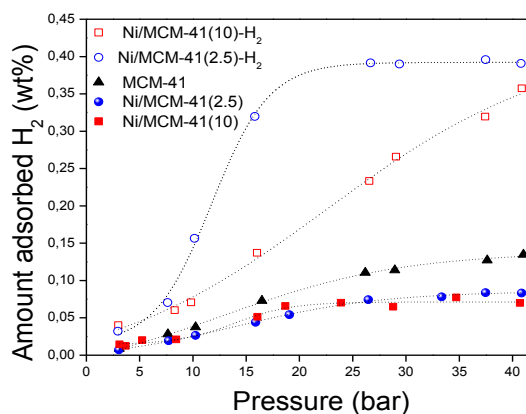


Figure 5. H₂ adsorption-desorption isotherms of the un-reduced and reduced samples at 293 K up to 40 bar.

At these conditions, the spillover effect could be possible. However, this phenomenon has not been demonstrated yet in samples of supported metals on non-reducible supports, such as silica (Prins 2012).

In order to explain the behavior of the Ni/MCM-41(2.5)-H₂ and Ni/MCM-41(10)-H₂ samples, and considering to the DFT calculations, one possible mechanism to be considered is the formation of nickel hydride between the reduced metal atoms and hydrogen molecules. This fact could explain the higher hydrogen stored on these samples than in MCM-41.

Finally, we propose that nickel, a relatively inexpensive metal, at low loadings and high dispersions could be used to increase the hydrogen storage capacity of silica materials at 77 K or 293 K (with different mechanisms involved). This fact

opens the possibilities of obtaining inexpensive and easily obtainable materials to achieve high hydrogen storages.

4. CONCLUSIONS

Ni/MCM-41 molecular sieves have been successfully prepared by wet impregnation. All of the materials exhibited high specific surface, pore volume and structural regularity typical of the MCM-41 mesoporous materials. The hydrogen adsorption on Ni/MCM-41 mesoporous materials at 77K was favoured for the low Ni loading, could be also associated to the presence of these highly dispersed Ni⁺² species which could give rise to hydrogen favorable sites. The reduced Ni/MCM-41 samples present higher H₂ storage at 293 K, which could be associated to the nickel hydrides formation.

Thus, MCM-41 mesoporous materials modified with nickel would be potentially suitable porous materials to H₂ storage.

5. REFERENCES

- Carraro, P.M., Elías, V.R., García Blanco, A.A., Sapag, K., Moreno, S., Oliva, M.I., Eimer, G.A. *Microporous Mesoporous Mater.* v.191, p.103–111, 2014.
- Carrott, P.J.M., Sing, K.S.W. *Surf. Sci. Catal.* v.39, p.77–87, 1988.
- Corma, A. *Chem. Rev.* v.97, p.2373–2420, 1997.
- Do, Y.J., Kim, J.H., Park, J.H., Park, S.S., Hong, S.S., Suh, C.S., Lee, G.D. *Catal. Today.* v.101, p.299–305, 2005.
- Elías, V.R., Crivello, M.E., Herrero, E.R., Casuscelli, S.G., Eimer, G.A. *J. Non. Cryst. Solids.* v.355, p.1269–1273, 2009.
- Hirscher, M.: *Handbook of Hydrogen Storage.* 2010.
- Jena, P. *J. Phys. Chem. Lett.* p.206–211, 2011.
- Liu, D., Lau, R., Borgna, A., Yang, Y. *Appl. Catal. A Gen.* v.358, p.110–118, 2009.



Park, S., Lee, S.Y. J. Colloid Interface Sci. v.346, p.194–198, 2010.

Prins, R. Chem. Rev. v.112 (5), p. 2714-2738, 2012.

Ramachandran, S., Ha, J.H., Kim, D.K. Catal. Commun. v.8, p.1934–1938, 2007.

Wu, C., Wang, L., Williams, P.T., Shi, J., Huang, J. Appl. Catal. B Environ. v.108-109, p.6–13, 2011.

Yang, J., Sudik, A., Wolverton, C., Siegel, D.J. Chem. Soc. Rev. v.39, p.656–75, 2010.

Züttel, A. Sci. Nat. v.91, p.157–72, 2004.